Published in final edited form as:
J Immunol. 2014 June 1; 192(11): 5059–5068. doi:10.4049/jimmunol.1400452.

Role of leukotriene A_4 hydrolase aminopeptidase in the pathogenesis of emphysema[1]

Mikell Paige[*], **Kan Wang**[†], **Marie Burdick**[‡], **Sunhye Park**[‡], **Josiah Cha**[‡], **Erin Jeffrey**[§], **Nicholas Sherman**[§], and **Y. Michael Shim**[‡]

[*]George Mason University, Department of Chemistry and Biochemistry, Manassas, VA

[†]Georgetown University Medical Center, Center for Drug Discovery, Washington, DC

[‡]University of Virginia, Department of Medicine, Division of Pulmonary and Critical Care Medicine, Charlottesville, VA

[§]Department of Microbiology, Immunology and Cancer Biology, University of Virginia, Charlottesville, VA

Abstract

The leukotriene A_4 hydrolase (LTA_4H) is a bi-functional enzyme with an epoxy hydrolase and aminopeptidase activities. We hypothesize that the LTA_4H aminopeptidase activity alleviates neutrophilic inflammation, which contributes to cigarette smoke (CS)-induced emphysema by clearing Proline-Glycine-Proline (PGP), a tri-amino acid chemokine known to induce chemotaxis of neutrophils. To investigate the biological contributions made by the LTA_4H aminopeptidase activity in CS-induced emphysema, we exposed wild type mice to CS over five months while treating them with a vehicle or a pharmaceutical agent (4MDM) that selectively augments the LTA_4H aminopeptidase without affecting the bio-production of leukotriene B_4 (LTB_4). Emphysematous phenotypes were assessed by *pre mortem* lung physiology with a small animal ventilator and by *postmortem* histologic morphometry. CS exposure acidified the airspaces and induced localization of the LTA_4H protein into the nuclei of the epithelial cells. This resulted in accumulation of PGP in the airspaces by suppressing the LTA_4H aminopeptidase activity. When the LTA_4H aminopeptidase activity was selectively augmented by 4MDM, the levels of PGP in the BALF and infiltration of neutrophils into the lungs were significant reduced without affecting the levels of LTB_4. This protected murine lungs from CS-induced emphysematous alveolar remodeling. In conclusion, CS exposure promotes the development of CS-induced emphysema by suppressing the enzymatic activities of the LTA_4H aminopeptidase in lung tissues and accumulating PGP and neutrophils in the airspaces. However, restoring the LTA_4 aminopeptidase activity with a pharmaceutical agent protected murine lungs from developing CS-induced emphysema.

Supported by the Flight Attendant Medical Research Institute (FAMRI YCSA to YMS), by the National Institute of Health (K08HL91127 to YMS), by the Ivy Foundation (Biomedical Research Grant to YMS).

Correspondence to: Y. M. Shim, M.D., PO BOX 800546, Division of Pulmonary and Critical Care Medicine, Department of Medicine, School of Medicine, University of Virginia, Charlottesville, VA 22908-0546. yss6n@virginia.edu. Phone: 434-924-5210. Fax: 434-924-9682.

Introduction

Leukotriene A_4 hydrolase (LTA_4H) has been known as a bi-functional enzyme. While two enzymatic activities share an overlapping substrate site, their biological functions are distinctive.(1, 2) The LTA_4H epoxy hydrolase (EH) converts leukotriene A_4 (LTA_4) to leukotriene B_4 (LTB_4), which is a potent inducer of neutrophil, macrophage, and T lymphocyte chemotaxisin human diseases.(3–10) The LTA_4H aminopeptidase degrades the n-terminus of peptides. Several studies demonstrated that a chemotactic tri-amino acid peptide, Proline-Glycine-Proline (PGP), is produced due to breakdown of collagen by prolyl-endopeptidase, and PGP has been shown to induce chemotaxis of neutrophils by binding to CXCR2.(11–19) Recently LTA_4H aminopeptidase has been reported to breakdown and clear PGP, thus, mitigating the influx of neutrophils into murine lungs *post* influenza infection.(20)

Pulmonary emphysema is a major manifestation of COPD. It is characterized by alveolar destruction in patients due to infiltration of neutrophils, lymphocytes, and macrophages into cigarette smoke (CS)-exposed lungs.(3, 8, 14, 21–23) Although a number of mechanisms were proposed to explain the pathogenesis of emphysema, its molecular pathogenesis is not yet clearly understood. Neutrophil-rich inflammation in emphysematous lungs of smokers led us to hypothesize that the LTA_4H aminopeptidase activity and bio-production/clearance of PGP may play an important role during the development of CS–induced neutrophilic inflammation and emphysema.

Our laboratory has previously reported that the LTA_4H enzymatic activities make important contribution to the development of emphysematous tissue alterations.(3, 24, 25) LTA_4H activity was found to influence severity of emphysematous alveolar remodeling in murine lungs exposed to transgenically over-expressedinterleukin-13.(3, 24) LTA_4H EH activity was found to contribute to emphysematous alveolar remodeling and neutrophilic infiltration into lungs *post* exposure of intra-nasal elastase.(3, 24) While a number of studies have characterized the importance of the LTA_4H EH, no studies have investigated the biological contributions made by the LTA_4H aminopeptidase during the development of emphysema. Therefore, we first investigated the CS-induced alterationsin the localization and enzymatic activity of the LTA_4H protein. These studies demonstrated that CS significantly increased the amount of LTA_4Hprotein in murine lungs and led to specific patterns of LTA_4H protein localization in lung tissues. Chronic exposure to CS also caused acidification of the bronchoalveolar lavage fluid (BALF) in mice, which suppressed the enzymatic activity of the LTA_4H aminopeptidase in the BALF. All of these events promoted exaggerated bio-production of PGP and LTB_4. When the activity of the LTA_4H aminopeptidase was restored by selectively augmenting it without changing the EH activity, murine lungs were protected from CS-induced emphysematous damage due to reduction in the levels of PGP and neutrophilic infiltration into the lungs without changes in the levels of LTB_4. These studies demonstrate that the LTA_4H aminopeptidase pathway is an important contributor for the CS-induced neutrophilic inflammation, PGP clearance, and emphysematous alveolar remodeling independent of the LTA_4H epoxy hydrolase pathway.

Materials and Methods

Formulation of 4MDM to improve water solubility and characterization of 4MDM bioavailability

The solubility of 4MDM was enhanced by formulation with 2-hydroxypropyl-β-cyclodextrin (CDX) and dextrose. The vehicle was prepared as an aqueous solution of CDX and dextrose without 4MDM. Maximum tolerated dose (MTD) was first determined with WT mice (n = 10) then the CDX-4MDM dose equal to 25% of the MTD was used in all subsequent *in vivo* studies. The solutions were administered as drinking water for mice in cages. The levels of 4MDM in BALF were quantified first by enriching 4MDM using C_{18} Sep-Pak (Waters Corp) then measuring the levels by using High Performance Liquid Chromatography equipped with a UV detector (HPLC-UV). The HPLC setup consisted of the following: Shimadzu CBM controller, Shimadzu LC20AD pump, Shimadzu SPD20A UV detector, Shimadzu CTO20A column oven, Waters C_{18} Symmetry HPLC column, and Shimadzu SIL20A auto injector. The Shimadzu EZ Start software was used to operate the instrument and for data analysis. The HPLC method parameters were as follows: binary conditions with a solvent rate of 1 mL/min for 15 minutes and simultaneous UV detection at $\lambda = 237$ nm. Each sample was injected twice. First, 100 μL of the unspiked samples was injected. Second, 90 μL of the samples spiked with 10 μL of known amounts of 4MDM were injected. Peaks corresponding to the 4MDM of each sample were identified by superimposing the 4MDM-spiked UV tracing onto the unspiked UV tracing of the samples. The levels of 4MDM were assessed by calculating the area under the curve of the BALF samples to known standard curves of 4MDM.

Cigarette Smoke-induced pulmonary emphysema

129sv wild type mice (WT) were purchased from National Cancer Institute. The LTA_4H knockout mice (LTA_4H KO) were provided by Dr. Beverly Koller (University of North Carolina).(26) Animal use was approved by the University of Virginia Institutional Animal Care and Use Committee. WT and LTA_4H knockout mice, 8 to 12 weeks of age, were exposed to cigarette smoke using a Teague TE-2 smoking apparatus. 3R4F research cigarettes were purchased from the University of Kentucky. Cigarettes were combusted at the rate of 3 cigarettes every 9 minutes, 5 hours a day, 5 days a week, over 5 months. Circulating air was trapped with an inline 22 μm filter attached to the air circulation system and total particulate matters were monitored in the air. Mice were studied 0, 1, 4, 20 weeks *post* exposure to cigarette smoke. Mice were exposed to either ambient air or cigarette smoke while being treated with either vehicle or a pharmaceutical agent (4MDM), which selectively augments the LTA_4H aminopeptidase activity without affecting the LTA_4H epoxy hydrolase activity.(25)

Pre-mortem pulmonary physiologic assessment

Total lung volume and lung compliance were assessed by the Flexivent (SCIREQ) as previously described.(3, 25, 27, 28) In brief, animals were deeply anesthetized with ketamine &xylazine mixture (60/5 mg per kg weight), the trachea was cannulated using p10 tubing, the sternum was opened, the diaphragm was cleared by opening the abdominal cavity, and animals were ventilated at a respiratory rate of 120 breaths per minute with

PEEP 3 cm H_2O per a pre-written macro program. This technique ensured that the live animals' voluntary effort could not influence the physiologic values detected by the Flexivent. Once the animals were acclimated to the Flexivent ventilator, the prescribed Flexivent algorithm was performed as previously described.(3, 25, 27,28), and the total lung volume and compliance were calculated using the software supplied with the ventilator. Animals were sacrificed following physiologic measurements, and tissues were harvested for *post-mortem* physiologic and morphometric assessment.

Post-mortem histological lung morphometry assessment

As previously described (3, 24, 25, 29), animals were anesthetized, the trachea was cannulated, and the lungs were removed *en block* and inflated at 25 cm H_2O pressure of 1% melted low-melting-point agarose gel (Promega) in PBS. The trachea was tied to keep the lungs inflated, and then fixed in 10 mL paraformaldehyde for 18 hours. The fixed lungs were stained with H&E. Alveolar size was determined by mean cordlength (L m) as previously described. (3, 24, 25, 29, 30) Sequential digital pictures (at least 10 per animal) of the entire lungs were captured by an Axiostar microscope (Carl Zeiss Microimaging), then processed by NIH Image 1.63 on a Macintosh computer with a macro downloaded from the NIH server user-macro directory (web link: http://rsb.info.nih.gov/nih-image/download/contrib/ChordLength.SurfaceArea).

Measurement of PGP in Broncholaveolar Lavage Fluid (BALF)

Quantitative analysis of PGP in the BALF by HPLC-MS proved to be highly unreliable presumably due to the matrix effects of the aromatic carbons generated from exposure to cigarette combustion. These aromatic carbons saturated the chromatography columns and made the columns unusable even after the first run of chromatography. Therefore, a two-step preparation of the BALF was performed as follows: First, the BALF was purified by normal flow HPLC. The retention time of a standard solution of PGP was determined in order to guide fractionation of PGP in the BALF samples. Second, the levels of PGP were quantified using a Thermo Electron TSQ Quantum Access MAX mass spectrometer system with a Protananospray ion source interfaced to a custom-packed 8 cm×75 um (internal diameter) Phenomenex Jupiter 10 um C_{18} reverse-phase capillary column. A 0.5 uL aliquot of each fractionated extract was injected, and the samples were eluted from the column using a reverse phase gradient from 0% to 100% acetonitrile at a flow rate of 0.5 μL/min over 0.5 hours. The nanospray ion source was operated at +3 kV. The MRM used was 270.2 – 172.9, 116.1.

In silico molecular modeling of LTA_4H, 4MDM, PGP, and LTA_4

The software Virtual Molecular Dynamics version 1.8.7 (VMD) was used to visualize and render the final figure.(31) The manual positioning of the ligands in the LTA_4H substrate-binding site was accomplished using the Molefracture Plugin version 1.3, which is available in the VMD package. The software GROMACS was used for energy minimization of the enzyme and ligands after solvation of the protein and ligands in a TIP3P water model.(32) The ligands were parameterized using the SwissParam server.(33) The minimization was carried out using the CHARMM27 force field, which is available in the GROMACS

package.(34) The E296Q mutant of the LTA_4H co-crystallized with the tripeptide Arg-Ala-Arg (PDB: 3B7T) was used as a template to build the Pro-Gly-Pro substrate in the peptidase-binding pocket of the enzyme.(35) A crystal structure of a wild-type LTA_4H (PDB: 3FTV) was used for all subsequent modeling of the protein.(36) On the basis of mutation data, the C-terminus carboxylate was positioned to form a hydrogen bond with the side chain of Arg563.(37) Hydrolysis of the peptide occurs at the N-terminus. Therefore, the N-terminal amine and the carboxyl oxygen were positioned to chelate with the Zn^{++} atom. The LTA_4, a precursor to LTB_4, was docked following mutation data. The substrate was arranged to set two hydrogen bonds between the Arg563 residue and the carboxylic acid moiety of LTA_4.(37)

Development of the LTA_4H ELISA

The concentration of the LTA_4H was determined by a custom-developed ELISA assay. Two LTA_4H antibodies were purchased from commercial vendors. The levels of LTA_4H in the BALF and lung homogenate soup were determined by using double-paired coating antibody (Novus EPR5713) and biotinylated detection antibody (R&D). Recombinant LTA_4H was purchased from Creative BioMart recombinant murine LTA_4H with His-tag as a standard. Fifty μL of samples were used in duplicates to quantify the amount of the LTA_4H. Samples were analyzed against the standard curve generated from known quantities of recombinant mouse LTA_4H enzyme. The ODs were measured with a Dynex Technology TRIAD ELISA reader controlled by Concert-Triad Serves software (version 2.0.0.12.) at a wavelength 450 nm for the measurement of LTA_4H.

FACS analysis of whole lung leukocyte infiltration

Whole lung single cell suspension was analyzed by FACS analysis with. Briefly mouse lungs were harvested then digested in lung digestion media with 1.0 mg/mL collagenase A (Roche Diagnostics) in RPMI (Quality Biological), and erythrocytes were lysed with ACK buffer (Quality Biological). Cells isolated from the lungs were stained with PerCP-labeled CD45 (BD), APC-Cy7-labeled CD11b (BD), PE-labeled Ly6G (BD), and FITC-Labeled LTA_4H (Bioss). Infiltrating leukocytes were gated from non-leukocytes by the expression of CD45. Next, all $CD45^{high}$ cells were gated into $Ly6G^{high}$ and $CD11b^{high}$ cells (neutrophils) as previously described.(3) For the purpose of detecting cells containing the LTA_4H in their intra-cellular space, cells were permeabilized with flow cytometry permeabilization buffer (R&D) after stained with CD45 antibody. Cells expressing LTA_4H were separated into two groups, leukocytes ($CD45^{high}$) and non-leukocytes ($CD45^{low}$). Multi-color detection of the stained cells was performed on a FACScan flow cytometer (BD Biosciences). FlowJo (version 8.8.6.) was used to analyze the data.

Evaluation of apoptosis in alveolar epithelial cells

Tunel stain was performed with TACS 2Td-DAB *in situ* apoptosis detection kit per manufacturer's protocol (Trevigen). Paraffin embedded lung blocks were at 8 μm thickness, then stained with reagents provided in the TACS 2Td-DAB kit. At least 5 animals in each group were studied. Ten adjacent pictures were taken from lungs of each animals at 40×

magnification power, positively stained epithelial cells (brown) were counted, then averaged to conduct statistical analyses.

LTA_4H immunohistochemistry

Immunohistochemistry was performed according to the commercial vendor's protocol (Vectostain Elite ABC kit) with Biogenex antigen retrieval citra plus, Biogenex power block, murine LTA_4H antibody and isotype control antibody (Novus), andDAB Vector peroxidase substrate kit.

Bronchoalveolar lavage fluid (BALF) collection and biochemical analysis

Animals were anesthetized as described above at specified time points, and BALF was collected and processed after pH was measured per previously published method.(3, 20, 24, 25) Concentration of the LTA_4H protein was determined by an ELISA assay developed in our laboratory. Concentrations of KC and MIP2 in BALF were determined by commercially available ELISA kits (R&D). Quantitative analysis of PGP in the BALF by HPLC-MS was achieved in two steps. First, BALF was purified by HPLC then PGP was quantified by a Thermo Electron TSQ Quantum Access MAX mass spectrometer system. Levels of LTB_4 were assessed by a commercially available LTB_4 EIA kit (R&D).(3, 24, 25)

Assessment of the LTA_4H Aminopeptidase activity

Recombinant human LTA_4H enzyme was produced, and the enzymatic properties of the LTA_4H aminopeptidase were assessed with a method previously published by our laboratory.(25) Twenty five μL BALF from each mouse was used to determine *in vivo* LTA_4H aminopeptidase activity.

Evaluation of metalloproteinase-8 and -9 (MMP8, MMP9)

Total RNA from lung tissue was isolated by Trizol.(3, 24, 25, 29, 30) Sybergreen real-time rt-PCR was performed then standardized with ²-actin to semi-quantify the genes transcribing for MMP8 and MMP9. Primers used for PCR are listed in the Table 1.

Statistics

All data were expressed as mean ± SEM and assessed for significance by t test or one-way ANOVA with Bonferroni subgroup comparison as appropriate. All statistics were performed using Prism software (GraphPad). In all analyses, p-value < 0.05 was considered significant.

Results

CS induced emphysematous tissue alteration in murine lungs

129sv WT mice developed progressively severe emphysematous tissue alteration with CS-exposure, and this was demonstrated by all three primary endpoints, *pre mortem* lung physiology (TLC &C_{st}) and *post mortem* histology (*L* m) (Figure 1).

Effects of CS on LTA_4H protein

Levels of the LTA_4H protein in the BALF and whole lung soup increased and peaked *post* 4 week CS-exposure. Then levels of the LTA_4H protein in the BALF of the CS-exposed mice decreased to the levels comparable to the age-matched, AA-exposed mice by 20 weeks (Figure 2A). However, levels of the LTA_4H protein in the whole lung protein soup of the CS-exposed mice were still significantly elevated as compared to the AA-exposed mice by 20 weeks (Figure 2B). Significantly more LTA_4H was found in intra-cellular staining of $CD45^+$ and $CD45^-$cells from the CS-exposed lungs as compared to AA-exposed lungs (Figure 2C). The LTA_4H protein was located in the cytosol of the airway epithelial cells in AA-exposed mice, but the LTA_4H protein was localized into the nuclei of the airway epithelial cells in CS-exposed mice (Figure 2D). Levels of $LTB_4$and PGP were significantly increased in the BALF of CS-exposed mice as compared to AA-exposed mice (Figure 3A and 3B). A significantly increased number of $CD45^{high}CD11b^{high}Ly6G^{high}$ cells infiltrated the CS-exposed lungs as compared to AA-exposed lungs (Figure 3C). BALF was found to be significantly more acidic in mice exposed to CS for 20 weeks (pH 6.7) as compared to mice exposed to AA for 20 weeks (pH 7.2) (Figure 3D). Enzymatic activity of the LTA_4H aminopeptidase was found to be significantly suppressed *in vitro* at pH 6.7 as compared to pH 7.2 (Figure 3E).

Developing a reagent to selectively augment the LTA_4Haminopeptidase without affecting LTA_4H EH activity

Previously we published the design and biological effects of 4MDM with which the LTA_4H aminopeptidase can be selectively augmented without affecting the EH activity.(25) However, its application was limited due to low water solubility. Therefore, we developed a water-soluble formulation of 4MDM by encapsulating it with 2-hydroxypropyl-β-cyclodextrin (CDX). The hydrophobic cavity of the CDX structure encapsulates the water-insoluble 4MDM while the hydrophilic exterior of the CDX affords a complex with improved water solubility (Figure 4A). A 4:1 molar ratio of CDX to 4MDM (CDX-4MDM) remained homogenous aqueous solution over a 72-hour (Table 2). After CDX-4MDM was administered to mice as drinking water mixed with dextrose (1 g dextrose per mL water), 4MDM was found in the BALF within 24 hours (Figure 4B). No mortality or gross abnormalities were observed after oral administration of CDX-4MDM for 5months (n=33).

Effects ofCDX-4MDM in CS-exposed mice

Molecular mechanism of selective augmentation of the LTA_4H aminopeptidase by 4MDM can be rationalized with a molecular model. *In silico* model of PGP and 4MDM in the substrate pocket of LTA_4H is presented with LTA_4in purple and 4MDM in orange (Figure 5A). The binding model for the 4MDM suggests that 4MDM augments the LTA_4H aminopeptidase by interacting with Phe314, and subsequently perturbing the chelation of Glu318 to the zinc atom and enhancing turnover of the peptide hydrolysis reaction.(38) The long aliphatic tail of $LTA_4$is predicted to extend into this pocket and preclude simultaneous binding of 4MDM. Therefore, 4MDM is not expected to alter LTA_4H EH activity, i.e. processing of $LTA_4$to LTB_4. *In vivo* effects of the CDX-4MDM were assessed by quantifying the levels of PGP and LTB_4. In CS-exposed mice treated with vehicle or

CDX-4MDM, levels of LTB_4 were not significantly different (Figure 5B). However, levels of PGP were significantly reduced in the mice treated with CDX-4MDM as compared to mice treated with vehicle *post* 20 week CS-exposure (Figure 5C). A significantly fewer number of $CD45^{high}CD11b^{high}Ly6G^{high}$ cells were found in the CS-exposed mice treated with CDX-4MDM as compared to CS-exposed mice treated with vehicle (Figure 5D). The selectivity of 4MDM at the LTA_4H enzyme target was confirmed by demonstrating that treatment with CDX-4MDM had no effects in mice with a *null* mutation at the LTA_4H *loci* (Figure 5E). After 20 week CS-exposure, assessment by *pre mortem* TLC and C_{st} and *post mortem L* m demonstrated that selective augmentation of the LTA_4H aminopeptidase activity protected lungs from CS-induced emphysematous alveolar tissue alteration (Figure 6).

Effects of 4MDM on the enzymatic activity of LTA_4H aminopeptidase in acidic environment

Effects of 4MDM on the enzymatic characteristics of the LTA_4H aminopeptidase at pH 6.7 were determined by using *in vitro* aminopeptidase activity assay with a previously published method.(25) The aminopeptidase activity was augmented with positive dose response to 4MDM (Figure 7A). The k_{cat} (enzymatic turn-over number) of the LTA_4H aminopeptidase increased from $17.2s^{-1}$in vehicle to $89.8s^{-1}$ in the presence of 8.0 μM 4MDMat pH 6.7 (Table 3). Treatment with 8.0 μM 4MDM at pH 6.7 increased the aminopeptidase activity by more than three folds as compared to treatment with vehicleat pH 7.2 (27.5/sec to 89.8/sec) (Table 3). Then the *in vivo* activity of the LTA_4H aminopeptidase was measured in the BALF. The specificity of this assay on measuring the LTA_4H aminopeptidase in the BALF was determine by demonstrating minimally detectable LTA_4H aminopeptidase activity in mice with null mutation at the LTA_4H *loci* as compared to mice with wild type LTA_4H *loci* (Figure 7B). The LTA_4H aminopeptidase activity was then found to be substantially augmented in the BALF from CS-exposed WT mice treated with oral CDX-4MDM as compared to CS-exposed WT mice treated with vehicle for 5 months (Figure 7C). These studies demonstrated that the loss of LTA_4H aminopeptidase activity caused by reduction in pH was rescued by treatment with CDX-4MDM which augmented the LTA_4H aminopeptidase activity with minimal off-targeting effects. Recovery of enzymatic activity indicates that at low pH, the LTA_4H protein is functionally suppressed but structurally intact.

In silico molecular modeling of LTA_4H, 4MDM, PGP, and LTA_4

In contrast to PGP, hydrolysis of LTA_4 is at the C-12 position and is stereo-selective to give exclusively the *R* epimer. Asp375 is an essential residue for this process, and presumably directs the addition of a water molecule to the C-12 carbon of the LTA_4 molecule.(37) Therefore, the LTA_4 in the LTA_4H substrate-binding pocket was assembled by positioning the *Re* face of the C-12 atom opposite the Asp375 residue. The 4MDM ligand was docked with the unsubstituted phenyl ring of 4MDM positioned to form pi-pi stacking interactions with the phenyl ring of Phe314 and the 4-methoxyphenyl substituent was positioned to interact with the hydrophobic side chain of Val367 through van der Waal interactions. The proposed binding mode is in accordance with the docking studies of Lai and co-workers on related analogs.(39)

Effects of CDX-4MDM on alveolar epithelial apoptosis

Mice after 20 week CS-exposure had a significantly higher number of alveolar epithelial cells staining positive in TUNEL assay as compared to AA-exposure (Figure 8). However, selective augmentation of the LTA_4H aminopeptidase significantly reduced apoptosis in CS-exposed mice as compared to CS-exposed, vehicle-treated mice.

Effects of CDX-4MDMon KC, MIP2, MMP8 and MMP9

PGP is known to bind to CXCR2and induces chemotaxis of neutrophils.(13, 19, 20, 40) Levels of KC in the BALF *post* CS-exposure were not significantly different between the mice treated with CDX-4MDM and vehicle (Figure 9A). However, levels of MIP2 in the BALF *post* CS-exposure were significant reduced in mice treated with CDX-4MDM as compared to mice treated with vehicle (Figure 9B). MMP8 and MMP9 have been found to be associated with PGP bio-production and subsequent infiltration of neutrophils into the diseased tissues.(12, 15, 18–20) Real time rt-PCR of the whole lung RNA demonstrated that the levels of genes transcribing for MMP8 and MMP9 were significantly increased *post* 20 week CS-exposure as compared to 20 week AA-exposure (Figure 9C & 9D). Levels of gene transcribing for MMP8 were not significantly altered *post* CS-exposure when compared between mice treated with vehicle or CDX-4MDM. However, selective augmentation of the LTA_4H aminopeptidase significantly reduced the levels of gene transcribing for MMP9 *post* 20 week CS-exposure as compared to vehicle treatment.

Discussion

An exaggerated activity of the LTA_4H enzyme frequently coexists with and is believed to contribute to the pathogenesis of a variety of diseases associated with neutrophils including sepsis, cystic fibrosis, non-steroid dependent asthma and COPD.(5, 41–45) Several studies have highlighted the importance of the exaggerated LTA_4HEH activity and its bio-product, LTB_4, which contribute to neutrophilic inflammation and tissue remodeling.(46–50) We have previously demonstrated that LTB_4 biosynthesis plays an important role in the emphysematous form of COPD induced by transgenic IL-13 and intra-nasally administered elastase.(24, 25) However, new evidence has emerged to suggest that the second enzymatic activity of the LTA_4H, namely the aminopeptidase, may play an important role involving its ability to break down and clear PGP, a product of collagen breakdown with chemotactic properties.

Our current studies provide further evidence to suggest that the LTA_4H aminopeptidase makes an important contribution to CS-induced neutrophilic inflammation and emphysema in lungs. First, we demonstrated that CS exposure alters the levels and distribution of the LTA_4H protein, which promote bio-production of LTB_4 and hinder clearance of PGP. After5-months ofCS-exposure, LTA_4H protein accumulated in the nuclei of the airway epithelial cells with minimal accumulation in the airspaces. Examination of the pH in the BALF after5-month CS-exposure demonstrated that CS-exposure acidified the BALF significantly (pH 6.7), and atpH6.7 the LTA_4H aminopeptidase activity was significantly suppressed than pH of the AA-exposed BALF (pH 7.2). We hypothesized that breakdown and clearance of PGP occurs primarily in the airspaces and that the bio-production of

LTB_4occurs primarily in nuclei where all necessary molecular components are present. Localization of the LTA_4H protein into nuclei and associated induction of LTB_4 bio-production have been described by others in the past.(51) Combination of these changes after CS-exposure was thought to create a cellular microenvironment in which persistently elevated levels of LTB_4 and PGP would occur.

Traditional transgenic strategies using knock-ins or knock-outs are limited due to the irinabilities to selectively modify the individual functions of the LTA_4Hbi-functional activities. All available pharmaceutical agents are limited because these agents are non-selective inhibitors of the LTA_4H EH and aminopeptidase. We overcame this limitation by developing4MDM which selectively augments the LTA_4Haminopeptidase without affecting the LTA_4H EH activity. This tool provided us with a new ability to probe the bi-functionality of the LTA_4H enzyme. We developed a water-soluble formulation for chronic administration suitable for a murine model of emphysema induced by chronic CS-exposure. We then demonstrated that selective augmentation of the LTA_4H aminopeptidase protects lungs from CS-induced emphysematous alveolar remodeling by enhancing the clearance of PGP and reducing neutrophilic inflammation independent of LTB_4 bio-production.

Our results demonstrated several notable observations related to the bi-functional activities of the $LTA_4H$and pathogenesis of emphysema. First, CS-exposure in pulmonary system induces complex bio-molecular alterations with in the bi-functional enzymatic activities of the LTA_4H protein. We demonstrated that CS-exposure causes distinctive localization of the LTA_4H protein in lung tissues and acidification of the airspaces which alter the LTA_4H aminopeptidase activity. These are, in our opinion, important bio-molecular events that have been previously underappreciated. Even though a number of animal studies showed promising pharmaceutical benefits by using LTA_4H inhibitors which indiscriminately block both enzymatic activities, no agents have been successfully translated to the bedside as FDA-approved therapeutics.(52–55) Our studies may provide additional biological in sights as to how these non-selective modifiers of the LTA_4H enzymatic activities may inadvertently cause unwanted and potentially harmful biological effects. This could occur by unknowingly canceling the “good” LTA_4H aminopeptidase while blocking the “bad” LTA_4H EH with non-selective LTA_4H modifiers. Localization of the LTA_4H protein into the nuclei also raises a possibility that the LTA_4H may potentially behave as a regulator of transcriptional factors such as MAPK or NF-κβ. This is an intriguing hypothesis which merits further investigation in the future.

Second, our molecular modeling and the properties of 4MDM suggest that the aminopeptidase activity of the $LTA_4H$is a druggable target. The challenge with targeting a multi-functional enzyme is modifying one activity of the enzyme without affecting the other activity. Selective augmentation of the aminopeptidase activity is possible because of the large substrate-binding pocket of the LTA_4Henzyme (Figure 5A). A number of available mutation data suggest that 4MDM would occupy the space between Val367 and Phe314 and form pi-pi stacking interaction with phenyl ring of Phe314 and van der Waal interactions with the hydrophobic side chain of Val367. In this model, 4MDM and PGP can simultaneously bind to the LTA_4H substrate site. Mutation data suggests that the aliphatic tail of LTA_4 must extend deep into the pocket, which would prevent simultaneous binding

with 4MDM. (37) It appears that this model offers a plausible explanation as to why 4MDM does not cause measurable changes in the LTA_4EH activity *in vivo*. Further studies involving co-crystallization of 4MDM with the LTA_4H is necessary to make a conclusive determination for its mechanism selective for aminopeptidase.

Third, the animals treated with CDX-4MDM showed reduction in the levels of MIP2 while the levels of KC were unchanged. This was an unanticipated epiphenomenon. Reactive oxygen species have been found to activate macrophages, and this interaction was found to induce neutrophil chemotaxis via production of MIP2.(56) We speculate that the selective augmentation of the LTA_4H aminopeptidase may alter interaction between alveolar macrophages and reactive oxygen species and reduce the levels of MIP2. This is a speculation that merits more studies in the future.

Fourth, CS-exposure up-regulated the genes transcribing for MMP8 and MMP9, which are described to contribute to the bio-production of PGP.(12, 15, 17, 57) Treatment with 4MDM selectively down-regulated the genes transcribing for MMP9 while it did not for MMP8. Previously others have reported that the MMP9 is potentially involved in a “feed-forward” mechanism, which perpetuates the *in vitro* bio-production of PGP due to CS-exposure.(12, 16) These findings suggest that the selective augmentation of the LTA_4H aminopeptidase could potentially halt this “feed-forward” cycle as a part of its therapeutic effects.

While CDX-4MDM provided an opportunity to probe the biology of the LTA_4H bi-functional activities, there are limitations in our study worthy mentioning. First, our current study appears to be potentially divergent from what we have observed in the LTA_4H KO animals.(3) In our previous study, we reported that the null mutation at the LTA_4H *loci* led to significant protection against emphysema induced by intra-nasal elastase administration. The elastase-induced model of emphysemaisone-hit model induced by a single-dose administration of porcine elastase. The CS-induced model of emphysema is repeated-insult model (daily smoking) induced over five months, and chronicity and repeating nature of the insults by CS likely induced pulmonary responses divergent from the elastase-induced model of emphysema. Second, all of our analyses were observational related to the development of emphysema and neutrophils. Secondary *in vivo* confirmation of our results would require depletion of neutrophils. Inherent limitations in available methods hindered this attempt. Mice with null mutation at the CXCR2 *loci* would alter non-neutrophil dependent biological mechanisms such as angiogenesis, which make important contributions to the pathogenesis of emphysema.(58–60) Neutrophil depletion with anti-Ly6G antibody was attempted in our laboratory for as long as one-month duration.(3) However, administration of this antibody longer than 1 months caused serum sickness in animals and was determined to be unsuitable for a chronic model like that of 20-week CS-exposure.

In summary, our studies highlighted cellular mechanisms associated with the perturbations in the bi-functional enzymatic activities of LTA_4H, which is responsible for emphysematous alveolar remodeling induced by CS-exposure. Our studies provided mechanistic insights that the development of the emphysematous destruction in lungs may be ameliorated by interventions that selectively regulate the LTA_4H aminopeptidase. This report features the unexplored bi-functional activities of the LTA_4H pathway as noteworthy sites for future

investigations designed to evaluate disease susceptibility, disease progression, and therapeutic utility in emphysema.

References

1. Thunnissen MM, Andersson B, Samuelsson B, Wong CH, Haeggstrom JZ. Crystal structures of leukotriene A4 hydrolase in complex with captopril and two competitive tight-binding inhibitors. FASEB J. 2002; 16:1648–1650. [PubMed: 12207002]
2. Andersson B, Kull F, Haeggstrom JZ, Thunnissen MM. Crystallization and X-ray diffraction data analysis of leukotriene A4 hydrolase from Saccharomyces cerevisiae. Acta Crystallogr D Biol Crystallogr. 2003; 59:1093–1095. [PubMed: 12777785]
3. Shim YM, Paige M, Hanna H, Kim SH, Burdick MD, Strieter RM. Role of LTB(4) in the pathogenesis of elastase-induced murine pulmonary emphysema. Am J Physiol Lung Cell Mol Physiol. 2010; 299:L749–L759. [PubMed: 20817777]
4. Stockley RA, Bayley DL, Unsal I, Dowson LJ. The effect of augmentation therapy on bronchial inflammation in alpha1-antitrypsin deficiency. Am J Respir Crit Care Med. 2002; 165:1494–1498. [PubMed: 12045122]
5. Hubbard RC, Fells G, Gadek J, Pacholok S, Humes J, Crystal RG. Neutrophil accumulation in the lung in alpha 1-antitrypsin deficiency. Spontaneous release of leukotriene B4 by alveolar macrophages. J Clin Invest. 1991; 88:891–897. [PubMed: 1653278]
6. Rios-Santos F, Benjamim CF, Zavery D, Ferreira SH, Cunha Fde Q. A critical role of leukotriene B4 in neutrophil migration to infectious focus in cecal ligaton and puncture sepsis. Shock. 2003; 19:61–65. [PubMed: 12558146]
7. Pace E, Profita M, Melis M, Bonanno A, Paterno A, Mody CH, Spatafora M, Ferraro M, Siena L, Vignola AM, Bonsignore G, Gjomarkaj M. LTB4 is present in exudative pleural effusions and contributes actively to neutrophil recruitment in the inflamed pleural space. Clin Exp Immunol. 2004; 135:519–527. [PubMed: 15008988]
8. Marian E, Baraldo S, Visentin A, Papi A, Saetta M, Fabbri LM, Maestrelli P. Up-regulated membrane and nuclear leukotriene B4 receptors in COPD. Chest. 2006; 129:1523–1530. [PubMed: 16778270]
9. Young RE, Voisin MB, Wang S, Dangerfield J, Nourshargh S. Role of neutrophil elastase in LTB4-induced neutrophil transmigration in vivo assessed with a specific inhibitor and neutrophil elastase deficient mice. Br J Pharmacol. 2007; 151:628–637. [PubMed: 17471175]
10. Grespan R, Fukada SY, Lemos HP, Vieira SM, Napimoga MH, Teixeira MM, Fraser AR, Liew FY, McInnes IB, Cunha FQ. CXCR2-specific chemokines mediate leukotriene B4-dependent recruitment of neutrophils to inflamed joints in mice with antigen-induced arthritis. Arthritis Rheum. 2008; 58:2030–2040. [PubMed: 18576322]
11. Overbeek SA, Braber S, Koelink PJ, Henricks PA, Mortaz E, LoTam Loi AT, Jackson PL, Garssen J, Wagenaar GT, Timens W, Koenderman L, Blalock JE, Kraneveld AD, Folkerts G. Cigarette smoke-induced collagen destruction; key to chronic neutrophilic airway inflammation? PLoS One. 2013; 8:e55612. [PubMed: 23383243]
12. Xu X, Jackson PL, Tanner S, Hardison MT, Abdul Roda M, Blalock JE, Gaggar A. A self-propagating matrix metalloprotease-9 (MMP-9) dependent cycle of chronic neutrophilic inflammation. PLoS One. 2011; 6:e15781. [PubMed: 21249198]
13. Jackson PL, Noerager BD, Jablonsky MJ, Hardison MT, Cox BD, Patterson JC, Dhanapal B, Blalock JE, Muccio DD. A CXCL8 receptor antagonist based on the structure of N-acetyl-proline-glycine-proline. Eur J Pharmacol. 2011
14. Braber S, Koelink PJ, Henricks PA, Jackson PL, Nijkamp FP, Garssen J, Kraneveld AD, Blalock JE, Folkerts G. Cigarette smoke-induced lung emphysema in mice is associated with prolyl endopeptidase, an enzyme involved in collagen breakdown. Am J Physiol Lung Cell Mol Physiol. 2011; 300:L255–L265. [PubMed: 21112944]
15. Gaggar A, Rowe SM, Matthew H, Blalock JE. Proline-Glycine-Proline (PGP) and High Mobility Group Box Protein-1 (HMGB1): Potential Mediators of Cystic Fibrosis Airway Inflammation. The open respiratory medicine journal. 2010; 4:32–38. [PubMed: 20448817]

16. O'Reilly PJ, Hardison MT, Jackson PL, Xu X, Snelgrove RJ, Gaggar A, Galin FS, Blalock JE. Neutrophils contain prolyl endopeptidase and generate the chemotactic peptide, PGP, from collagen. J Neuroimmunol. 2009; 217:51–54. [PubMed: 19875179]

17. O'Reilly P, Jackson PL, Noerager B, Parker S, Dransfield M, Gaggar A, Blalock JE. N-alpha-PGP and PGP, potential biomarkers and therapeutic targets for COPD. Respir Res. 2009; 10:38. [PubMed: 19450278]

18. Lin M, Jackson P, Tester AM, Diaconu E, Overall CM, Blalock JE, Pearlman E. Matrix metalloproteinase-8 facilitates neutrophil migration through the corneal stromal matrix by collagen degradation and production of the chemotactic peptide Pro-Gly-Pro. Am J Pathol. 2008; 173:144–153. [PubMed: 18556780]

19. Weathington NM, van Houwelingen AH, Noerager BD, Jackson PL, Kraneveld AD, Galin FS, Folkerts G, Nijkamp FP, Blalock JE. A novel peptide CXCR ligand derived from extracellular matrix degradation during airway inflammation. Nat Med. 2006; 12:317–323. [PubMed: 16474398]

20. Snelgrove RJ, Jackson PL, Hardison MT, Noerager BD, Kinloch A, Gaggar A, Shastry S, Rowe SM, Shim YM, Hussell T, Blalock JE. A critical role for LTA4H in limiting chronic pulmonary neutrophilic inflammation. Science. 2010; 330:90–94. [PubMed: 20813919]

21. Hautamaki RD, Kobayashi DK, Senior RM, Shapiro SD. Requirement for macrophage elastase for cigarette smoke-induced emphysema in mice. Science. 1997; 277:2002–2004. [PubMed: 9302297]

22. Bracke KR, D'Hulst A I, Maes T, Moerloose KB, Demedts IK, Lebecque S, Joos GF, Brusselle GG. Cigarette smoke-induced pulmonary inflammation and emphysema are attenuated in CCR6-deficient mice. J Immunol. 2006; 177:4350–4359. [PubMed: 16982869]

23. D'Hulst A I, Vermaelen KY, Brusselle GG, Joos GF, Pauwels RA. Time course of cigarette smoke-induced pulmonary inflammation in mice. Eur Respir J. 2005; 26:204–213. [PubMed: 16055867]

24. Shim YM, Zhu Z, Zheng T, Lee CG, Homer RJ, Ma B, Elias JA. Role of 5-lipoxygenase in IL-13-induced pulmonary inflammation and remodeling. J Immunol. 2006; 177:1918–1924. [PubMed: 16849505]

25. De Oliveira EO, Wang K, Kong HS, Kim S, Miessau M, Snelgrove RJ, Shim YM, Paige M. Effect of the leukotriene A4 hydrolase aminopeptidase augmentor 4-methoxydiphenylmethane in a pre-clinical model of pulmonary emphysema. Bioorg Med Chem Lett. 2011; 21:6746–6750. [PubMed: 21983441]

26. Byrum RS, Goulet JL, Snouwaert JN, Griffiths RJ, Koller BH. Determination of the contribution of cysteinyl leukotrienes and leukotriene B4 in acute inflammatory responses using 5-lipoxygenase- and leukotriene A4 hydrolase-deficient mice. J Immunol. 1999; 163:6810–6819. [PubMed: 10586081]

27. Jonasson S, Hedenstierna G, Hedenstrom H, Hjoberg J. Comparisons of effects of intravenous and inhaled methacholine on airway physiology in a murine asthma model. Respir Physiol Neurobiol. 2009; 165:229–236. [PubMed: 19136080]

28. Martin EL, Sheikh TA, Leco KJ, Lewis JF, Veldhuizen RA. Contribution of alveolar macrophages to the response of the TIMP-3 null lung during a septic insult. Am J Physiol Lung Cell Mol Physiol. 2007; 293:L779–L789. [PubMed: 17586692]

29. Zhu Z, Homer RJ, Wang Z, Chen Q, Geba GP, Wang J, Zhang Y, Elias JA. Pulmonary expression of interleukin-13 causes inflammation, mucus hypersecretion, subepithelial fibrosis, physiologic abnormalities, and eotaxin production. J Clin Invest. 1999; 103:779–788. [PubMed: 10079098]

30. Zhu Z, Ma B, Zheng T, Homer RJ, Lee CG, Charo IF, Noble P, Elias JA. IL-13-induced chemokine responses in the lung: role of CCR2 in the pathogenesis of IL-13-induced inflammation and remodeling. J Immunol. 2002; 168:2953–2962. [PubMed: 11884467]

31. Humphrey W, Dalke A, Schulten K. VMD: visual molecular dynamics. J Mol Graph. 1996; 14:33–38. 27–38. [PubMed: 8744570]

32. Van Der Spoel D, Lindahl E, Hess B, Groenhof G, Mark AE, Berendsen HJ. GROMACS: fast, flexible, and free. J Comput Chem. 2005; 26:1701–1718. [PubMed: 16211538]

33. Zoete V, Cuendet MA, Grosdidier A, Michielin O. SwissParam: a fast force field generation tool for small organic molecules. J Comput Chem. 2011; 32:2359–2368. [PubMed: 21541964]

34. Bjelkmar P, Larsson P, Cuendet MA, Hess B, Lindahl E. Implementation of the CHARMM Force Field in GROMACS: Analysis of Protein Stability Effects from Correction Maps, Virtual Interaction Sites, and Water Models. J Chem Theory Comput. 2010; 6:459–466.

35. Tholander F, Muroya A, Roques BP, Fournie-Zaluski MC, Thunnissen MM, Haeggstrom JZ. Structure-based dissection of the active site chemistry of leukotriene A4 hydrolase: implications for M1 aminopeptidases and inhibitor design. Chem Biol. 2008; 15:920–929. [PubMed: 18804029]

36. Davies DR, Mamat B, Magnusson OT, Christensen J, Haraldsson MH, Mishra R, Pease B, Hansen E, Singh J, Zembower D, Kim H, Kiselyov AS, Burgin AB, Gurney ME, Stewart LJ. Discovery of leukotriene A4 hydrolase inhibitors using metabolomics biased fragment crystallography. J Med Chem. 2009; 52:4694–4715. [PubMed: 19618939]

37. Rudberg PC, Tholander F, Andberg M, Thunnissen MM, Haeggstrom JZ. Leukotriene A4 hydrolase: identification of a common carboxylate recognition site for the epoxide hydrolase and aminopeptidase substrates. J Biol Chem. 2004; 279:27376–27382. [PubMed: 15078870]

38. Jiang X, Zhou L, Wu Y, Wei D, Sun C, Jia J, Liu Y, Lai L. Modulating the substrate specificity of LTA4H aminopeptidase by using chemical compounds and small-molecule-guided mutagenesis. Chembiochem. 2010; 11:1120–1128. [PubMed: 20432426]

39. Jiang X, Zhou L, Wei D, Meng H, Liu Y, Lai L. Activation and inhibition of leukotriene A4 hydrolase aminopeptidase activity by diphenyl ether and derivatives. Bioorg Med Chem Lett. 2008; 18:6549–6552. [PubMed: 18952425]

40. Hardison MT, Brown MD, Snelgrove RJ, Blalock JE, Jackson P. Cigarette smoke enhances chemotaxis via acetylation of proline-glycine-proline. Front Biosci (Elite Ed). 2012; 4:2402–2409. [PubMed: 22652647]

41. Martin TR, Pistorese BP, Chi EY, Goodman RB, Matthay MA. Effects of leukotriene B4 in the human lung. Recruitment of neutrophils into the alveolar spaces without a change in protein permeability. J Clin Invest. 1989; 84:1609–1619. [PubMed: 2553777]

42. Bailie MB, Standiford TJ, Laichalk LL, Coffey MJ, Strieter R, Peters-Golden M. Leukotriene-deficient mice manifest enhanced lethality from Klebsiella pneumonia in association with decreased alveolar macrophage phagocytic and bactericidal activities. J Immunol. 1996; 157:5221–5224. [PubMed: 8955165]

43. Wardlaw AJ, Hay H, Cromwell O, Collins JV, Kay AB. Leukotrienes, LTC4 and LTB4, in bronchoalveolar lavage in bronchial asthma and other respiratory diseases. J Allergy Clin Immunol. 1989; 84:19–26. [PubMed: 2546985]

44. Friedrich EB, Tager AM, Liu E, Pettersson A, Owman C, Munn L, Luster AD, Gerszten RE. Mechanisms of leukotriene B4--triggered monocyte adhesion. Arterioscler Thromb Vasc Biol. 2003; 23:1761–1767. [PubMed: 12947016]

45. Fretland DJ, Widomski DL, Anglin CP, Penning TD, Yu S, Djuric SW. Leukotriene B4-induced granulocyte trafficking in guinea pig dermis. Effect of second-generation leukotriene B4 receptor antagonists, SC-50605 and SC-51146. Inflammation. 1993; 17:353–360. [PubMed: 8392493]

46. Izquierdo JL, Almonacid C, Parra T, Perez J. [Systemic and lung inflammation in 2 phenotypes of chronic obstructive pulmonary disease]. Arch Bronconeumol. 2006; 42:332–337. [PubMed: 16945263]

47. Kostikas K, Gaga M, Papatheodorou G, Karamanis T, Orphanidou D, Loukides S. Leukotriene B4 in exhaled breath condensate and sputum supernatant in patients with COPD and asthma. Chest. 2005; 127:1553–1559. [PubMed: 15888827]

48. Beeh KM, Kornmann O, Buhl R, Culpitt SV, Giembycz MA, Barnes PJ. Neutrophil chemotactic activity of sputum from patients with COPD: role of interleukin 8 and leukotriene B4. Chest. 2003; 123:1240–1247. [PubMed: 12684317]

49. Woolhouse IS, Bayley DL, Stockley RA. Sputum chemotactic activity in chronic obstructive pulmonary disease: effect of alpha(1)-antitrypsin deficiency and the role of leukotriene B(4) and interleukin 8. Thorax. 2002; 57:709–714. [PubMed: 12149532]

50. Hill AT, Campbell EJ, Bayley DL, Hill SL, Stockley RA. Evidence for excessive bronchial inflammation during an acute exacerbation of chronic obstructive pulmonary disease in patients

with alpha(1)-antitrypsin deficiency (PiZ). Am J Respir Crit Care Med. 1999; 160:1968–1975. [PubMed: 10588615]

51. Brock TG, Lee YJ, Maydanski E, Marburger TL, Luo M, Paine R 3rd, Peters-Golden M. Nuclear localization of leukotriene A4 hydrolase in type II alveolar epithelial cells in normal and fibrotic lung. Am J Physiol Lung Cell Mol Physiol. 2005; 289:L224–L232. [PubMed: 15805137]
52. Schmitt-Grohe S, Zielen S. Leukotriene receptor antagonists in children with cystic fibrosis lung disease : anti-inflammatory and clinical effects. Paediatric drugs. 2005; 7:353–363. [PubMed: 16356023]
53. Roberts WG, Simon TJ, Berlin RG, Haggitt RC, Snyder ES, Stenson WF, Hanauer SB, Reagan JE, Cagliola A, Tanaka WK, Simon S, Berger ML. Leukotrienes in ulcerative colitis: results of a multicenter trial of a leukotriene biosynthesis inhibitor, MK-591. Gastroenterology. 1997; 112:725–732. [PubMed: 9041233]
54. Hawkey CJ, Dube LM, Rountree LV, Linnen PJ, Lancaster JF. A trial of zileuton versus mesalazine or placebo in the maintenance of remission of ulcerative colitis. The European Zileuton Study Group For Ulcerative Colitis. Gastroenterology. 1997; 112:718–724. [PubMed: 9041232]
55. Usery JB, Self TH, Muthiah MP, Finch CK. Potential role of leukotriene modifiers in the treatment of chronic obstructive pulmonary disease. Pharmacotherapy. 2008; 28:1183–1187. [PubMed: 18752388]
56. Kawamura H, Kawamura T, Kanda Y, Kobayashi T, Abo T. Extracellular ATP-stimulated macrophages produce macrophage inflammatory protein-2 which is important for neutrophil migration. Immunology. 2012; 136:448–458. [PubMed: 22564028]
57. Kong MY, Gaggar A, Li Y, Winkler M, Blalock JE, Clancy JP. Matrix metalloproteinase activity in pediatric acute lung injury. Int J Med Sci. 2009; 6:9–17. [PubMed: 19159011]
58. Matsuo Y, Raimondo M, Woodward TA, Wallace MB, Gill KR, Tong Z, Burdick MD, Yang Z, Strieter RM, Hoffman RM, Guha S. CXC-chemokine/CXCR2 biological axis promotes angiogenesis in vitro and in vivo in pancreatic cancer. Int J Cancer. 2009; 125:1027–1037. [PubMed: 19431209]
59. Belperio JA, Keane MP, Burdick MD, Gomperts B, Xue YY, Hong K, Mestas J, Ardehali A, Mehrad B, Saggar R, Lynch JP, Ross DJ, Strieter RM. Role of CXCR2/CXCR2 ligands in vascular remodeling during bronchiolitis obliterans syndrome. J Clin Invest. 2005; 115:1150–1162. [PubMed: 15864347]
60. Addison CL, Daniel TO, Burdick MD, Liu H, Ehlert JE, Xue YY, Buechi L, Walz A, Richmond A, Strieter RM. The CXC chemokine receptor 2, CXCR2, is the putative receptor for ELR+ CXC chemokine-induced angiogenic activity. J Immunol. 2000; 165:5269–5277. [PubMed: 11046061]

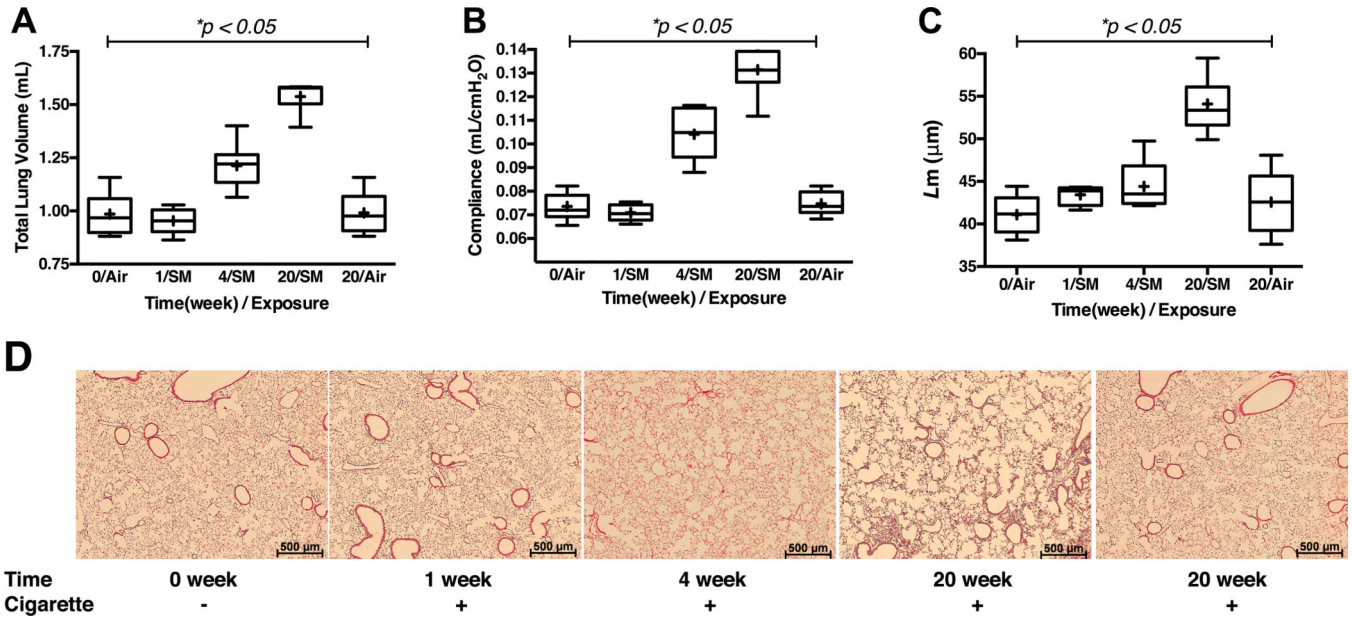

Figure 1.

Assessment of the emphysema phenotype in 129sv wild type mice *post* exposure to cigarette smoke by Teague TE-2 smoking apparatus over 5 months. **Panel A:** *Pre* mortem total lung volume measured by Sireq Flexivent. **Panel B:** *Pre mortem* quasi-static lung compliance measured by Sireq Flexivent. **Panel C:** *Post mortem* alveolar *L* m. **Panel D:** Representative H&E histology of the lungs at low power (2.5× magnification). Time = duration of exposure to cigarette smoke. Cigarette dose = 3 cigarettes per 9 minutes, 5 hours a day, 5 days a week. * represents analysis by ANOVA. N = 9–13 animals per groups in panels A and B. N = 5 animals per group in panel C.

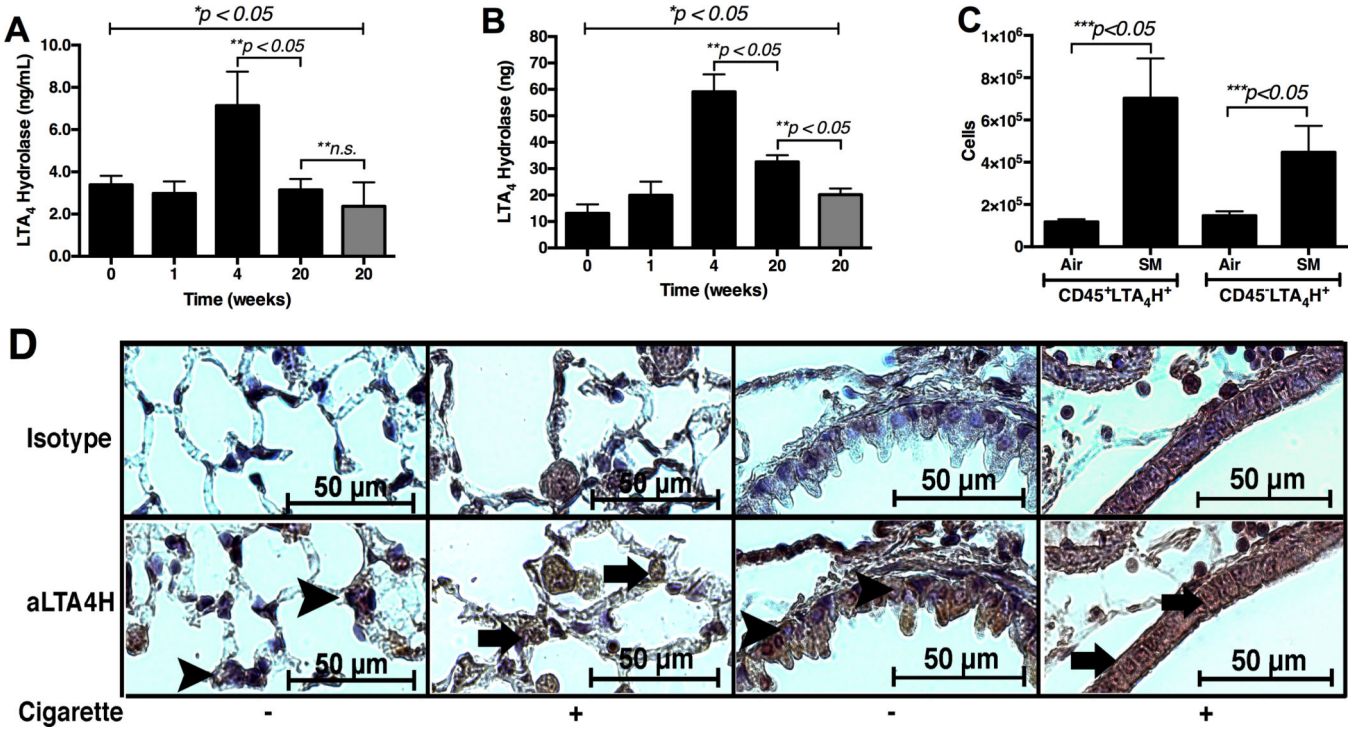

Figure 2.

Assessment of the LTA_4H protein expression in 129sv wild type mice *post* exposure to cigarette smoke over 5 months. **Panel A:** The levels of LTA_4H protein in the whole lung BALF assessed by ELISA. **Panel B:** The levels of LTA_4H protein in the whole lung protein soup assessed by ELISA. **Panel C:** Flow cytometry of the whole lung single cell suspension. Air = mice exposed to ambient air for 20 weeks. SM = mice exposed to cigarette smoke for 20 weeks. **Panel D:** Immunohistochemistry with antibody specific to murine LTA_4H protein in lung tissues from mice exposed to cigarette smoke for 20 weeks (63× oil magnification). Positive signals appear brown and counterstained with blue. Arrowheads show nuclei with positive counterstain (blue) indicating absence of LTA_4H protein. Arrows show nuclei with positive stain (grown) indicating presence of LTA_4H protein. Gray bars in Panels A & B = ambient-air exposed mice with ages 26 – 28 weeks. * represents analysis by ANOVA, ** by Bonferroni subgroup comparison, and *** by nonparametric t-Test. N = 5 per group.

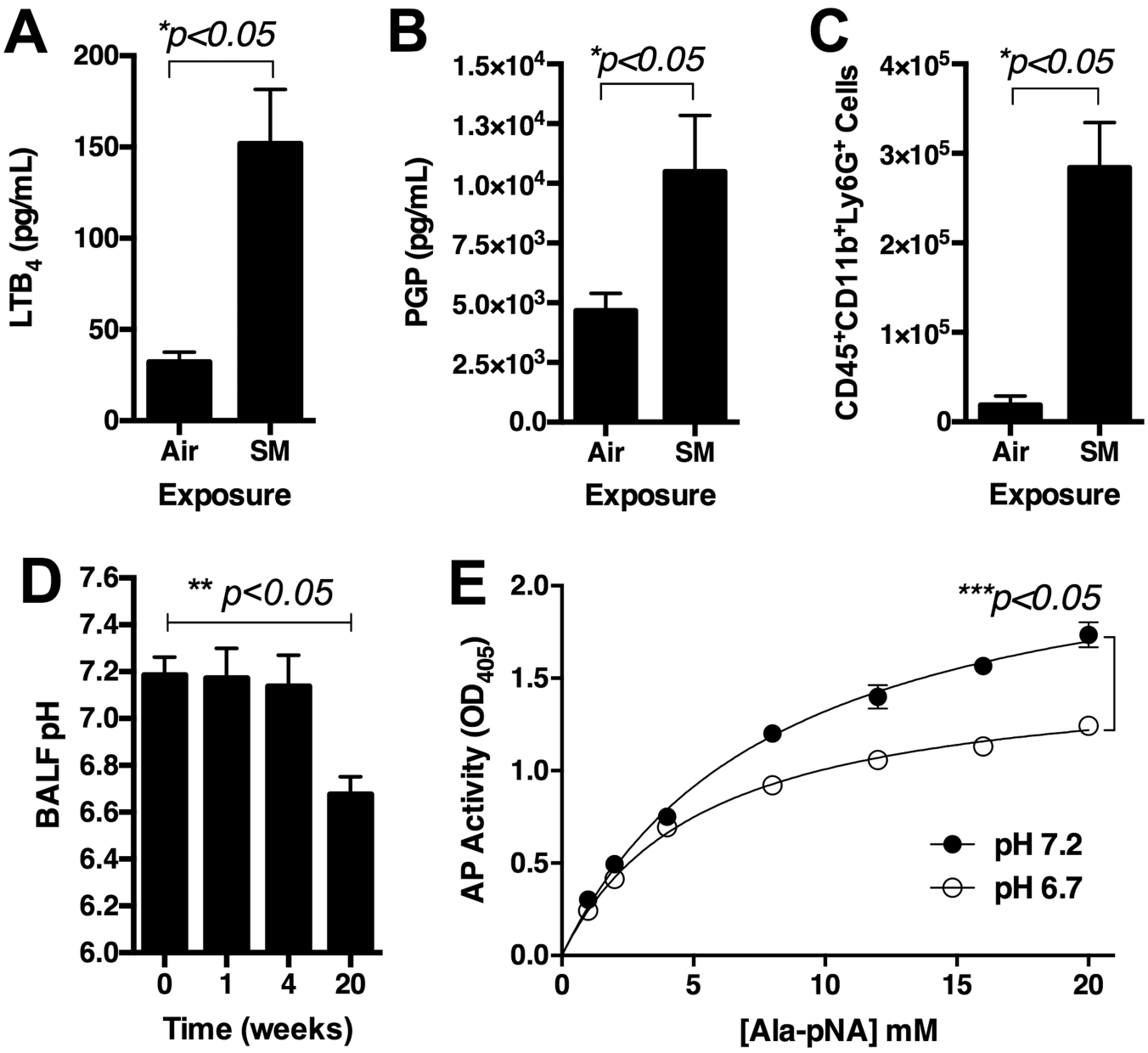

Figure 3.

Assessment of 129sv wild type mice *post* exposure to cigarette smoke by Teague TE-2 smoking apparatus for 5 months. **Panel A:** Levels of LTB_4 in BALF. **Panel B:** Levels of PGP in BALF. **Panel C:** Levels of $CD45^+CD11b^+Ly6G^+$ cells in whole lung single cell suspension. Antibodies are with PerCP-labeled CD45, ACP-labeled CD11b, and PE-labeled Ly5G. **Panel D:** pH of BALF over 20-week cigarette smoke exposure. **Panel E:** *In vitro* aminopeptidase activity assay using human recombinant LTA_4H at pHs 6.7 and 7.2. * represents analysis by nonparametric t-Test. ** represents analysis by ANOVA.*** represents two-way ANOVA with AP activity and time as two factors. N = 5 per group. Air = ambient air exposure. SM = cigarette smoke exposure.

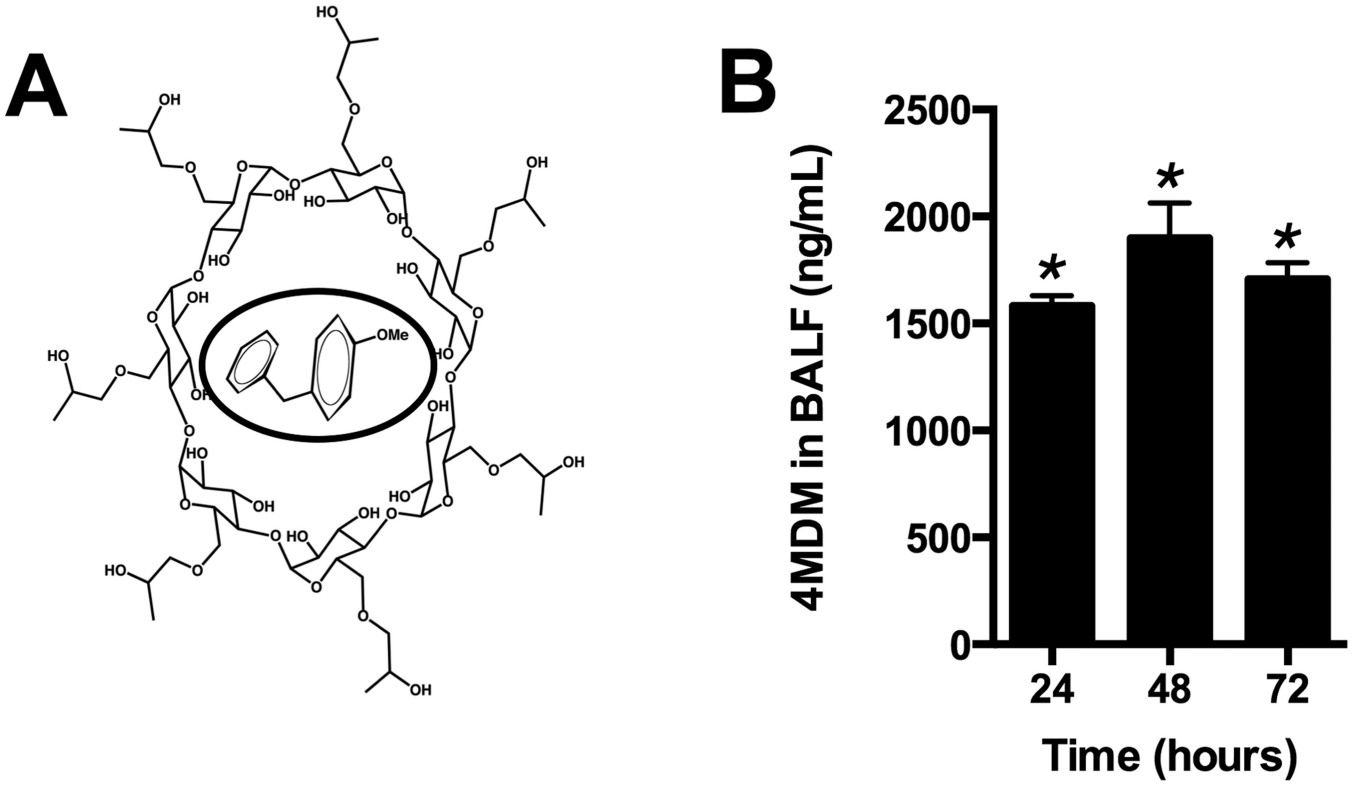

Figure 4.

Panel A: Diagram of CDX encapsulating 4MDM. 4MDM is in the inner pocket of CDX and highlighted with an oval circle. **Panel B:** Levels of 4MDM in BALF 24, 48, and 72 hours after CDX-4MDM was started to be administered as drinking water in mice. * represents column statistics comparing the levels of 4MDM to the hypothetical value of untreated mice, in this case, 0 ng/mL. N = 5 animals per group.

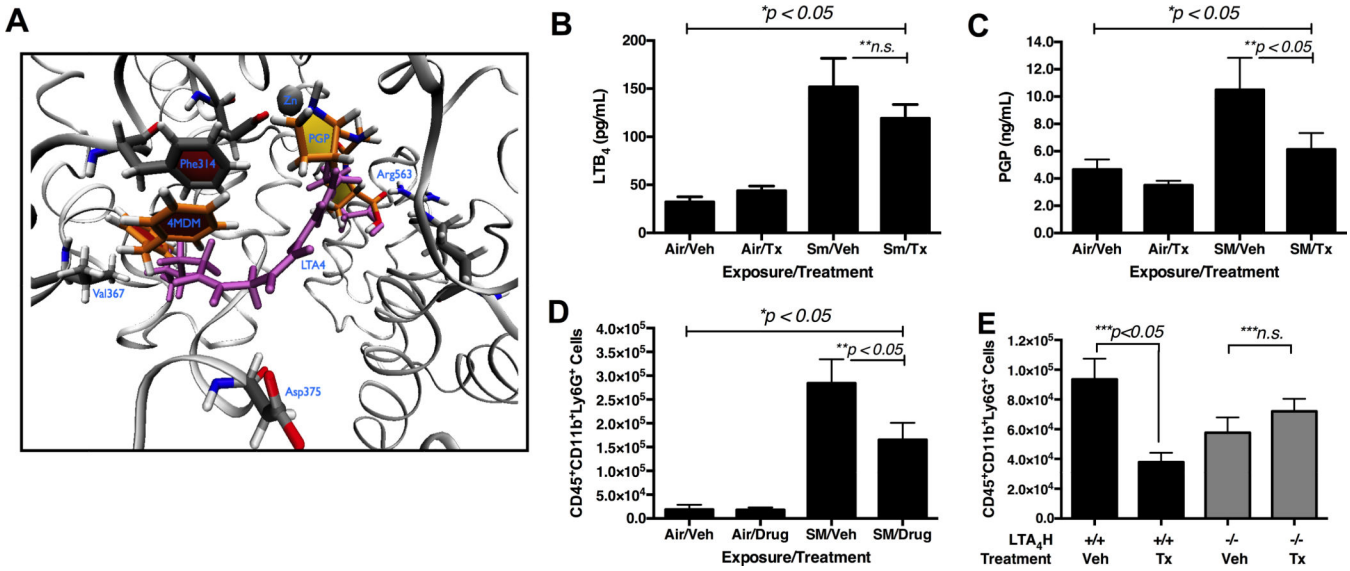

Figure 5.

Effects of CDX-4MDM treatment on the levels of LTB_4, PGP, and neutrophils in mice exposed to cigarette smoke for 20 weeks. **Panel A:** *In silico* modeling of the LTA_4H binding pocket occupied by 4MDM and PGP overlaid with the predicted binding model of the LTA_4. 4MDM = orange. PGP = yellow. LTA_4 = purple. **Panel B:** Levels of LTB_4 in BALF with oral CDX-4MDM or vehicle treatment *post* exposure to cigarette smoke for 20 weeks. **Panel C:** Levels of PGP in BALF with oral CDX-4MDM or vehicle treatment *post* exposure to cigarette smoke for 20 weeks. **Panel D:** Levels of $CD45^+CD11b^+Ly6G^+$ cells in whole lung single cell suspension with oral CDX-4MDM or vehicle treatment *post* exposure to cigarette smoke for 20 weeks. **Panel E:** Levels of $CD45^+CD11b^+Ly6G^+$ cells in whole lung single cell suspension of 129sv WT mice (black bars) and 129sv mice with null mutation at the LTA_4H *loci* (gray bars) with oral CDX-4MDM or vehicle treatment *post* exposure to cigarette smoke for 7 days. * represents analysis by ANOVA, ** by Bonferroni subgroup comparison, and *** by nonparametric t-Test. N = 5 – 6 per group.

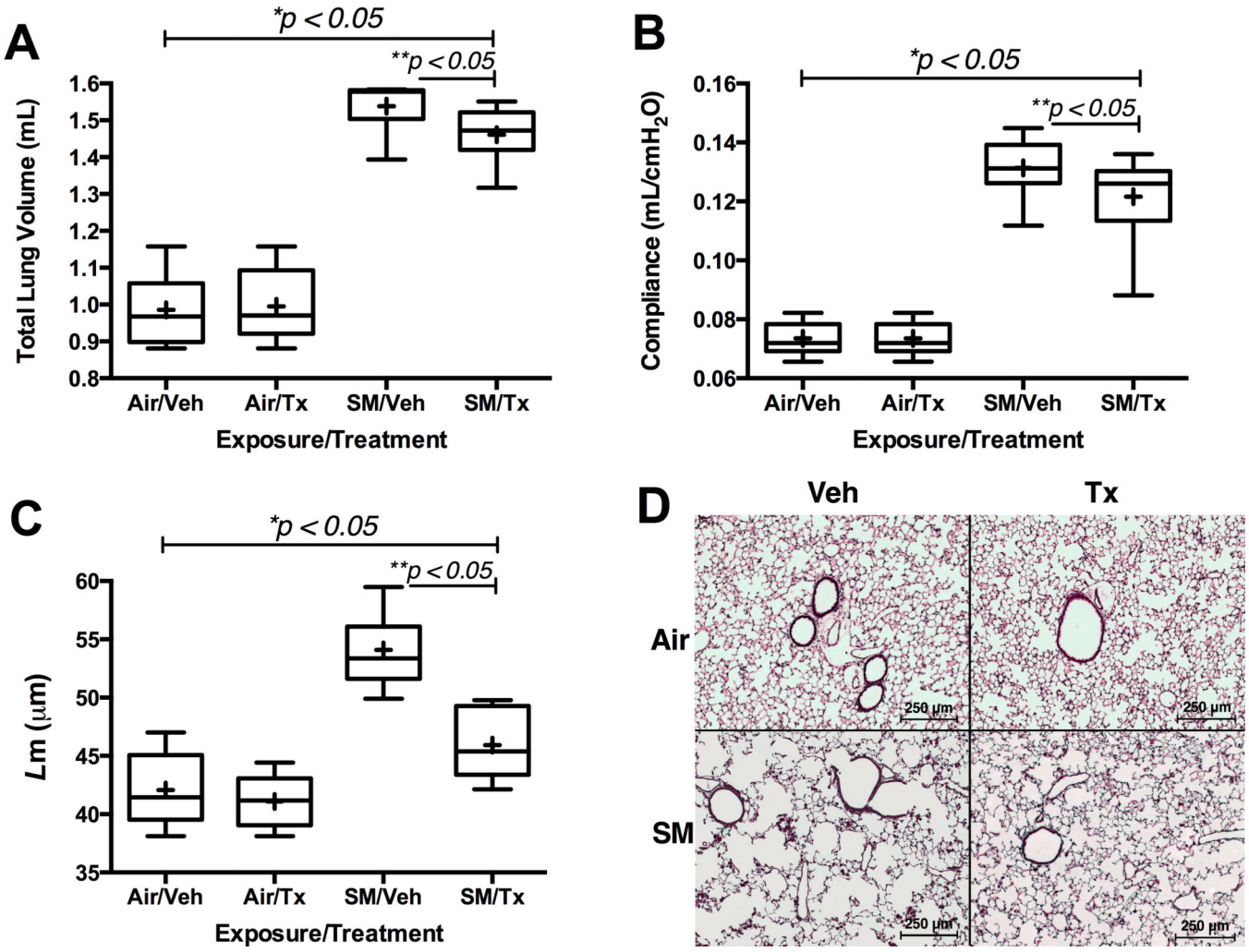

Figure 6.

Effects of CDX-4MDM treatment on pulmonary emphysema in WT mice exposed to cigarette smoke or ambient air for 20 weeks. **Panel A:** *Pre* mortem total lung volume measured by Sireq Flexivent. Total lung volume was measured after inflating the lungs with 30 cm H_2O pressure. **Panel B:** *Pre mortem* quasi-static lung compliance measured by Sireq Flexivent. **Panel C:** *Post mortemL* m. **Panel D:** Representative H&E histology of the lungs (10× magnification). + in the box and whisker plot represents mean while horizontal bar represents median. * represents analysis by ANOVA, and ** by Bonferroni subgroup comparison. N = 9–13 animals per groups in panels A and B. N = 5 animals per group in panels C.

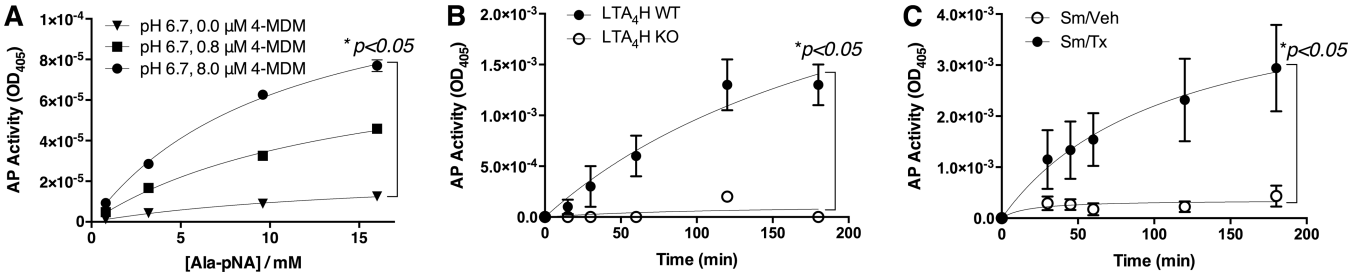

Figure 7.

LTA_4H aminopeptidase activity assay. **Panel A.** *In vitro* LTA_4H aminopeptidase activity assay with human recombinant LTA_4H in the presence of increasing doses of 4MDM at culture medium pH 6.7. AP activity is assessed by UV light absorption at $\lambda = 405$. **Panel B.** LTA_4H aminopeptidase activity assay with BAL fluid collected from mice with wild type (WT) or null mutation (LTA_4H KO) at the LTA_4H *loci*. N = 5 per group. **Panel C.** LTA_4H aminopeptidase activity assay with BALF fluid collected from mice treated with vehicle or 4MDM after exposure to cigarette smoke for 20 weeks. N = 6 per group. All data points are mean ± SEM. * represents two-way ANOVA with AP activity as the first factor and 4MDM dose (Panel A) or time (Panels B & C) as the second factor.

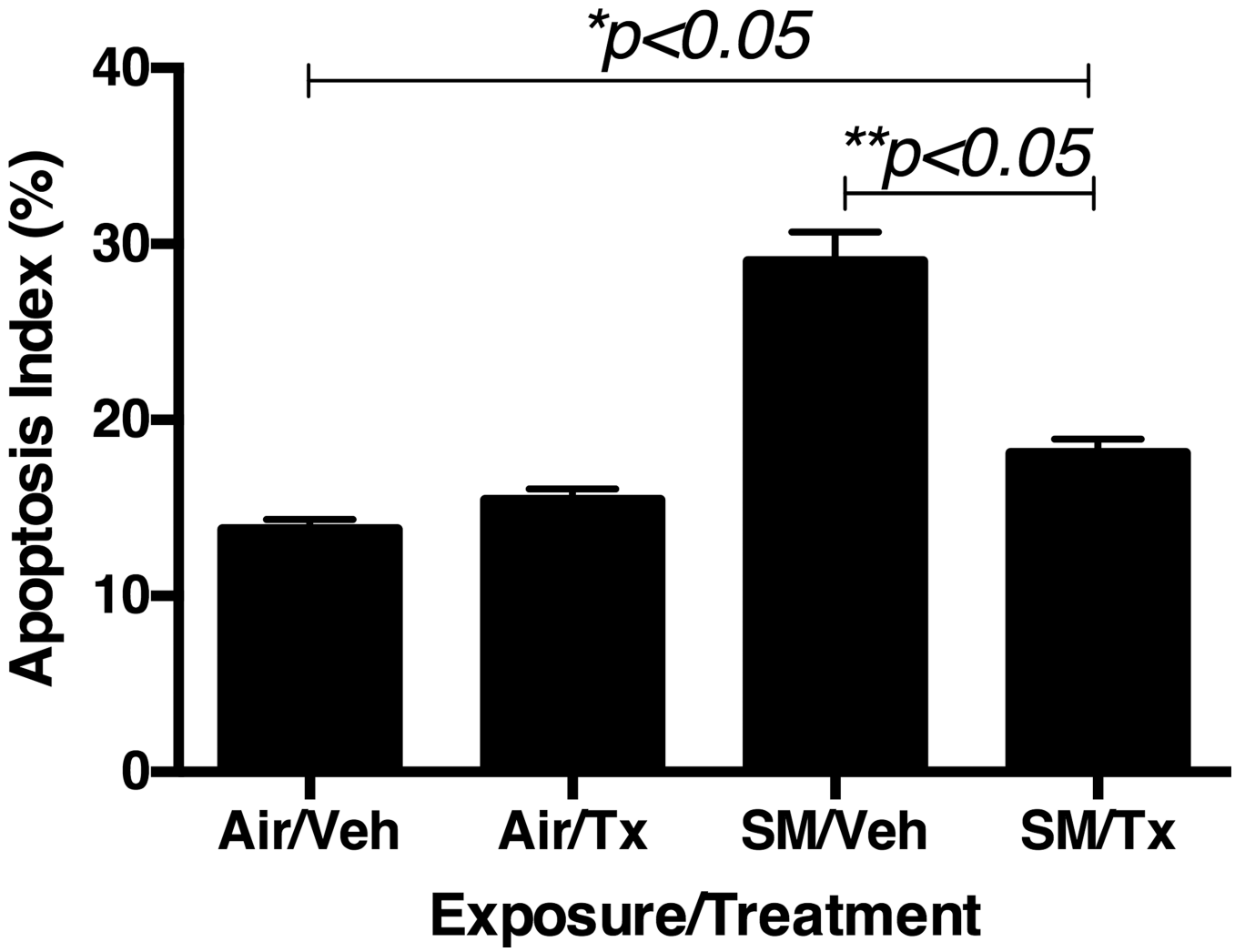

Figure 8.

Effects of CDX-4MDM treatment on apoptosis in WT mice exposed to cigarette smoke or ambient air for 20 weeks. Counting of TUNEL positive cells and calculating Apoptosis Index (percentage of cells positively stained in TUNEL assay). Ten random pictures of each animal were examined. N = 5 per group. Air = ambient air exposure. SM = cigarette smoke exposure. Veh = CDX containing vehicle. Tx = CDX-4MDM. * represents analysis by ANOVA, and ** by Bonferroni subgroup comparison.

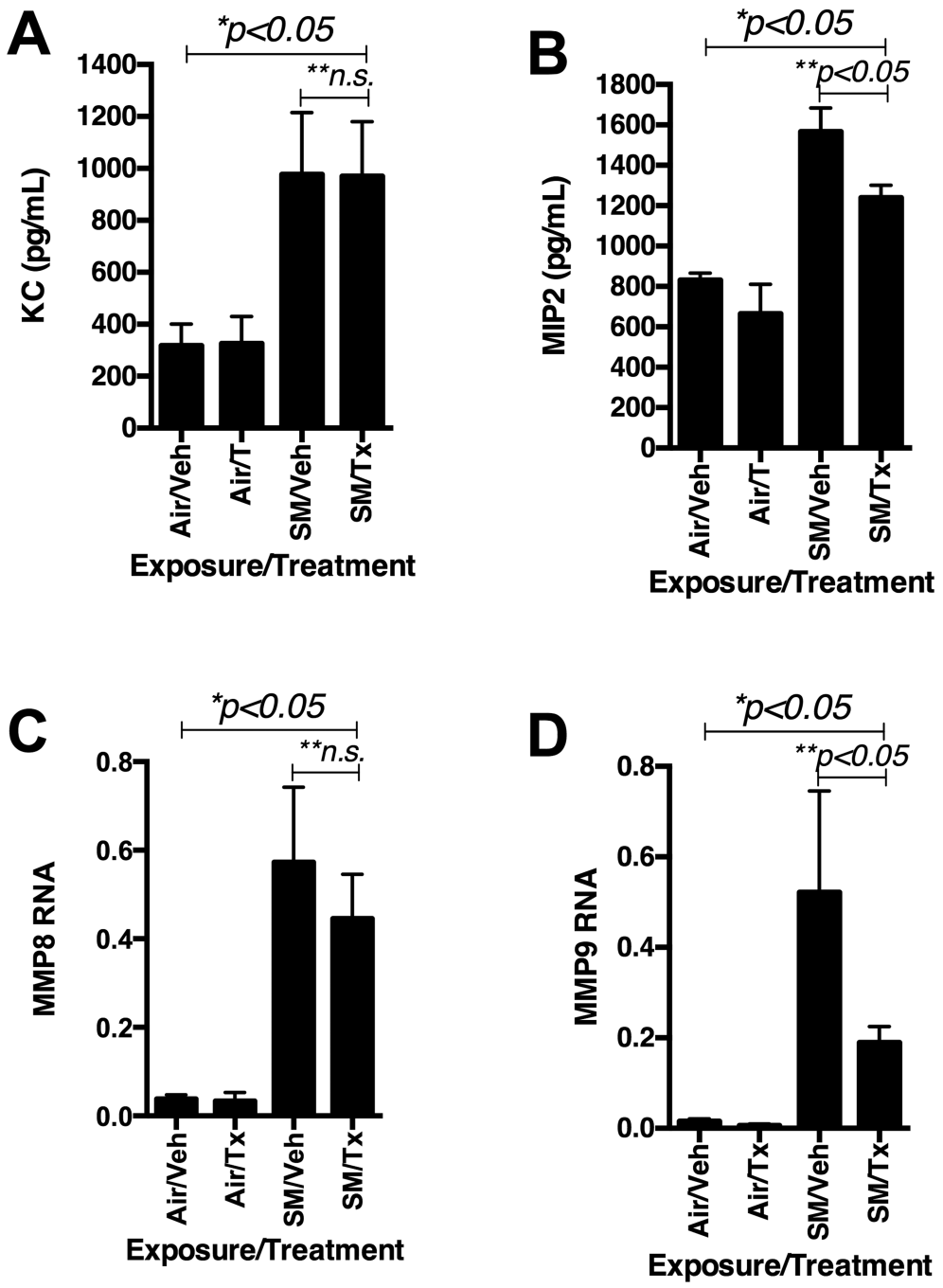

Figure 9.

Effects of CDX-4MDM treatment on WT mice exposed to cigarette smoke or ambient air for 20 weeks. **Panel A:** Levels of KC in the BALF from WT mice exposure to cigarette smoke for 20 weeks. **Panel B:** Levels of MIP2 in the BALF from WT mice exposure to cigarette smoke for 20 weeks. **Panel C:** Levels of RNA transcribing for MMP8 in whole lung RNA isolate normalized by β-actin. **Panel D:** Levels of RNA transcribing for MMP9 in whole lung RNA isolate normalized by β-actin. * represents analysis by ANOVA and ** by

Bonferroni subgroup comparison. N = 5–7 animals per groups. Air = ambient air exposure. SM = cigarette smoke exposure. Veh = CDX containing vehicle. Tx = CDX-4MDM.

Table 1

Primer sets for real time PCR.

Gene	AT[1]	Left Primer	Right Primer
β-actin	60 °C	AGCCATGTACGTAGCCATCC	CTCTCAGCTGTGGTGGTGAA
MMP8	60 °C	CCCACCTGAGATTTGATGCT	CTGAAGACCGTTGGGTAGGA
MMP9	60 °C	CAATCCTTGCAATGTGGATG	AGTAAGGAAGGGGCCCTGTA

[1] AT = annealing temperature

Table 2

Stability of a water-soluble formulation of 4MDM.[1]

Time (hours)	CDX:4MDM ratio	4MDM concentration (mM)
0	4:1	5.20 (100%)
48	4:1	4.82 (92.7%)
72	4:1	4.45 (85.6%)

[1] Levels of 4MDM in CDX-4MDM formulation kept at room temperature up to 72 hours.

Table 3

Effect of 4MDM on LTA_4H aminopeptidase activity.

	pH 7.2	**pH 6.7**	**pH 6.7**	**pH 6.7**
4MDM	0.0 μM	0.0 μM	0.8 μM	8.0 μM
k_{cat}[1]	27.5 ± 1.12	17.2 ± 2.24	59.3 ± 6.10	89.8 ± 6.26
K_M[2]	7.66 ± 0.74	16.30 ± 3.99	14.51 ± 2.69	10.83 ± 1.53

[1] k_{cat} = enzymatic turnover (s^{-1})

[2] K_M = concentration at one-half maximum velocity (mM)